AD-A052 806 HARVARD COLL OBSERVATORY CAMBRIDGE MASS CENTER FOR AS--ETC F/G 3/2
MODELS FOR THE SOLAR TRANSITION LAYER,(U)
MAR 78 G L WITHBROE F19628-76-C-0281
UNCLASSIFIED PREPRINT-902 AFGL-TR-78-0067 NL

END
DATE FILMED
5 78
DDC

UNCLASSIFIED

SECURITY CLASSIFICATION OF THIS PAGE (When Data Entered)

(19) REPORT DOCUMENTATION PAGE

READ INSTRUCTIONS BEFORE COMPLETING FORM

(18) 1. REPORT NUMBER: AFGL-TR-78-0067	2. GOVT ACCESSION NO.
3. RECIPIENT'S CATALOG NUMBER	
(6) 4. TITLE (and Subtitle): Models for the Solar Transition Layer	5. TYPE OF REPORT & PERIOD COVERED: Scientific [redacted]-2
(14) 6. PERFORMING ORG. REPORT NUMBER: Preprint [redacted]-982,	
(10) 7. AUTHOR(s): George L. Withbroe	(15) 8. CONTRACT OR GRANT NUMBER(s): F19628-76-C-0281
9. PERFORMING ORGANIZATION NAME AND ADDRESS: Center for Astrophysics, Smithsonian Institute, 60 Garden Street, Cambridge, Massachusetts 02138	10. PROGRAM ELEMENT, PROJECT, TASK AREA & WORK UNIT NUMBERS: 62101F; (16) 464303AS; (17) 03
11. CONTROLLING OFFICE NAME AND ADDRESS: Air Force Geophysics Laboratory, Hanscom AFB, MA 01731, Contract Monitor: D. Guidice/PHP	(11) 12. REPORT DATE: Mar [redacted]78
	13. NUMBER OF PAGES: 14
14. MONITORING AGENCY NAME & ADDRESS (if different from Controlling Office)	15. SECURITY CLASS. (of this report): Unclassified
(12) 16p.	15a. DECLASSIFICATION/DOWNGRADING SCHEDULE

16. DISTRIBUTION STATEMENT (of this Report)

Approved for public release; distribution unlimited.

17. DISTRIBUTION STATEMENT (of the abstract entered in Block 20, if different from Report)

18. SUPPLEMENTARY NOTES

19. KEY WORDS (Continue on reverse side if necessary and identify by block number)

Solar transition layer	Temperature-density structure
Transition layer model	Mechanical energy deposition
Transition region properties	OSO-8 Workshop, 1-10 Nov 77

20. ABSTRACT (Continue on reverse side if necessary and identify by block number)

Empirical and theoretical models of the transition layer are discussed. Theoretical models based on the assumption that there is a balance between the mechanical energy deposition and the radiative and conductive fluxes appear to be consistent with empirical results. The configuration of the magnetic field appears to have a major effect on the temperature-density structure for the transition layer. Models which intend to represent the physical conditions in the transition layer must take this into consideration, as well as including the

DD FORM 1 JAN 73 1473 EDITION OF 1 NOV 65 IS OBSOLETE

UNCLASSIFIED

SECURITY CLASSIFICATION OF THIS PAGE (When Data Entered)

409 956

20. Abstract (continued)

effects of small-scale inhomogeneities and mass flow.

Center for Astrophysics
Preprint Series No. 902

MODELS FOR THE SOLAR TRANSITION LAYER

George L. Withbroe

Center for Astrophysics
Harvard College Observatory and Smithsonian Astrophysical Observatory
Cambridge, Massachusetts 02138

MODELS FOR THE SOLAR TRANSITION LAYER

George L. Withbroe

Harvard - Smithsonian
Center for Astrophysics

ABSTRACT

Empirical and theoretical models for the transition layer are discussed. Theoretical models based upon the assumption that there is a balance between the mechanical energy deposition and the radiative and conductive fluxes appear to be consistent with empirical results. The configuration of the magnetic field appears to have a major effect on the temperature-density structure of the transition layer. Models which intend to repesent the physical conditions in the transition layer must take this into consideration, as well as including the effects of small scale inhomogeneities and mass flows.

1. Introduction

Knowledge of the physical conditions in the solar transition region is important for a variety of reasons. The transition layer is the interface through which mass and energy flow between the chromosphere and corona. The transport of energy by thermal conduction into the transition layer is a primary coronal cooling mechanism. A reliable determination of the magnitude of energy lost by this mechanism depends on knowledge of the temperature gradients in the transition layer. This layer may also play a major role in determining the mass flow between the chromosphere and corona. Current empirical and theoretical models suggest that there may be a unique relationship between the temperature gradient and density in the transition layer, a relationship specified by the requirement that the mechanical energy, radiative and conductive fluxes be in balance. In order to achieve this balance the atmosphere responds to changes in mechanical energy deposition in the transition layer and corona by increasing or decreasing the temperature gradients and densities in these layers. Consequently, it appears possible that the transition layer not only acts as an interface in the flow of mass and energy between the chromosphere and corona, but also exerts some control over the magnitude of these flows.

Since there have been a number of reviews (e.g. Jordan 1975, 1976; Gabriel 1977, Kopp and Orrall 1977, White 1977, Withbroe 1977a, Withbroe and Noyes 1977, Zirker 1977) that have summarized recent observations and models for the transition layer, the present paper will discuss only certain aspects of current empirical and theoretical models and the limitations of these models.

2. Empirical Models

Information about the physical conditions in the transition layer can be derived from extreme ultraviolet (EUV) observations made with instruments carried above the terrestrial atmosphere and from measurements of radio brightness temperatures at centimeter and decimeter wavelengths. For most purposes the EUV data are more useful than radio data because of the superior spatial resolution of recent EUV observations and variety of diagnostic techniques that can be applied to the analysis of these measurements.

One of the parameters that can be derived from EUV observations with a minimum number of assumptions is the differential emission measure Q(T) defined by

$$\int Q(T)\, dT = \int N_e^2\, dV. \qquad (1)$$

The differential emission measure gives the number of electrons

in the volume V characterized by temperatures between T and T+dT. The intensity of an EUV spectral line is given by (Pottasch 1964, 1967; Withbroe 1970)

$$I(\mathrm{erg/cm^2/sec/ster}) = 1.7\times10^{-16}\, Af\int N_e^2 gG(T)dh \qquad (2)$$

where A is the chemical abundance, relative to hydrogen, of the element forming the line; f is the oscillator strength; g is the Gaunt factor; and G(T) is a temperature-dependent term depending on the excitation and ionization properties of the atom producing the line. Abundances used in the present analysis are from Withbroe (1976), Gaunt factors from Bely (1966), ionization equilibrium calculations from Allen and Dupree (1969) and Dupree and Wood (1969), and the other parameters from Dupree (1972)

If we define V to be the volume along the line of sight above one square centimeter of solar surface, then dV=dh and

$$I = 1.7\times10^{-16}\, Af\int Q(T)gG(T)dT \qquad (3)$$

from equations (1) and (2). If one has measurements of the intensities of a number of lines whose functions gG(T) span different temperature regimes, one can obtain estimates of the differential emission measure from these measurements and equation (3) (see Withbroe 1975).

Figure 1 illustrates the differential emission measure obtained from a mean quiet sun spectrum given by Vernazza and Reeves (1977). This spectrum is an average over both network and cell regions. The individual points in Figure 1 are values of $\langle Q(T_f)\rangle$ obtained from equation (3) by assuming Q(T) is constant over the region of line formation for a given line which is assumed to have a mean temperature of formation T_f equal to the temperature where its function gG(T) has its maximum value. A better estimate of the differential emission measure can be obtained by various iterative techniques (e.g. Jordan and Wilson 1971, Jordan 1975, Withbroe 1975) to obtain a solution for Q(T) that reproduces the observed intensities when used in equation (3). An iterative solution is plotted as a solid line in Figure 1. In regions where the differential emission measure varies rapidly with temperature, utilization of mean values $\langle Q(T_f)\rangle$ gives a poor representation for the actual differential emission measure, as shown, for example, by the data for log T<5.0, where the actual temperatures of formation are lower than log T_f by about 0.1 dex because of the steep gradient in Q(T) for log T<5.0.

Not all of the lines whose mean values of $Q(T_f)$ are plotted in Figure 1 were used in deriving the empirical

differential emission measure curve. Only those lines with wavelengths longer than 912Å (points) or which are strong lines in the lithium isoelectronic sequence (squares) were utilized. Equation (2) assumes that the EUV lines originate in two level atoms where all of the electrons are in the ground level. This is an adequate assumption for the lithium isoelectronic sequence. However, many EUV lines are from isoelectronic sequences (such as the beryllium and boron sequences) which have low lying metastable levels which can have appreciable populations, in some cases equal to that in the ground level (cf. Jordan and Wilson 1971, Munro et al. 1971, Dupree 1972). Yet, even if the lowest lying values of $\langle Q(T_f) \rangle$ in Figure 1 are moved upward by 0.1 to 0.3 dex in order to correct for the effects of metastable levels, they will still fall systematically below the adopted differential emission measure curve given by the solid line. All of the low lying points have wavelengths shortward of 912Å. Since the geometrical thickness of the transition layer is very thin, of the order of a few hundred to a thousand kilometers for log $T \lesssim 5.6$, a significant fraction of the radiation from these lines could be absorbed by low lying cool inhomogeneties (e.g. spicules, dark mottles, fibrils, etc.) which are opaque due to absorption in the hydrogen Lyman continuum. Similar effects have been found in prominences (cf. Noyes et al., 1972). This explanation also accounts for some of the peculiarities observed in the limb brightening of lines with wavelengths less than 912Å, such as O IV λ554 (cf. Withbroe and Mariska 1976).

Another possible explanation for the systematic differences between the low lying points and adopted emission measure curve in Figure 1 is that the lithium isoelectronic sequence gives abnormally large values for Q(T) because of systematic errors in the ionization equilibrium calculations for this sequence (Jordan 1977). We will assume in this paper that the emission measure differences are caused by the combined effects of metastable populations and Lyman continuum absorption, and thus that the adopted emission measure curve is the appropriate one to use in deriving models. However, this problem needs further investigation.

Figure 2 presents differential emission measure curves for several different types of regions, including a representative active region, network and cell areas in a quiet region, and a coronal hole. The spectra utilized in deriving these curves are from Vernazza and Reeves (1977). Since the radiative loss per square centimeter of surface in each of these regions is given by

$$E_r = \int N_e N_H \phi(T) dh = 0.8 \int Q(T) \phi(T) dT \qquad (4)$$

for a fully ionized plasma, where $\phi(T)$ is the radiative loss function (cf. Cox and Tucker 1969, Raymond et al. 1976, McWhirter et al. 1975), these curves indicate that the radiative losses in the transition layer increase systematically as one moves from cell areas in quiet regions to network regions to active regions. The curves also indicate that the radiative losses in the transition layers of quiet regions and coronal holes are nearly the same.

In principle if one has a measurement of the density at some height in the transition layer and assumes hydrostatic equilibrium and a geometry (e.g. plane parallel), then one can determine the variation of the temperature and density with height in the transition layer (see review by Jordan, 1975). One important parameter is the electron pressure which does not vary significantly with height in the lower transition layer (log $T \lesssim 5.7$) because the pressure scale height is much smaller than the geometrical thickness of the layer. Electron pressures can be estimated by a variety of techniques. One can use spectroscopic data to determine pressures in the chromosphere and corona and thus the pressure in the transition layer, if all three layers are in hydrostatic equilibrium. One can also obtain estimates from optical depths derived from limb brightening observations and from density-sensitive line ratios for EUV lines formed in the transition layer. One can also compare the observations with theoretical models, particularly certain types of energy balance models (see section 3). Tables I and II list representative pressures $P/k = N_e T$ obtained by these techniques.

Let us examine first the data from the network and cell areas. Some of the pressure determinations indicate that the pressures in these areas are essentially the same, while others suggest that the pressure is higher in the network. It is not obvious which determinations are more reliable, consequently we cannot draw firm conclusions about similarities or differences between the temperature-density structures of network and cell areas. If the pressures are the same, then the emission measures (see Figure 2), which are proportional to $p^2 (dT/dh)^{-1}$, imply that the temperature gradient in the network is on the average a factor of 2 to 3 shallower than in cells. However, if the pressure in the network is larger by a factor of 2 or more, as indicated by some of the values given in Table I, then the temperature gradient in the network is steeper by a factor of 2 to 3 than in the cells. This problem needs further investigation.

For the active region whose differential emission measure is given in Figure 2 one finds empirically that the pressure is about 5 times that in the quiet region (see Table II), and thus that the temperature gradient is steeper than in the quiet region by a factor of about 2.5. For the energy balance model where the ratio of the active region to quiet region pressures is 10, the ratio of the temperature gradients is also 10.

Since the empirical values for the electron pressures in

TABLE I. ELECTRON PRESSURES IN QUIET REGIONS

TECHNIQUE	Log P/k = log $N_e T$ AVERAGE	CELL	NETWORK	SOURCE
CHROMOSPHERE	14.7-14.9			Vernazza (1977b)
CORONA				
Limb Observations (White light and EUV)	14.8			Mariska (1977)
Disk Observations	14.9	14.9	14.9	Mariska (1977)
TRANSITION LAYER				
Optical Depths*				
C II λ1335				
(ξ = 0)	$\gtrsim$14.2		$\gtrsim$14.3	Mariska (1977); Withbroe, Mariska (1976)
(ξ = 17 km/sec)	$\gtrsim$13.8		$\gtrsim$14.0	
C III λ977				
(ξ = 0)	$\gtrsim$14.5		$\gtrsim$14.7	Mariska (1977); Withbroe, Mariska (1976)
(ξ = 17 km/sec)	$\gtrsim$14.2		$\gtrsim$14.4	
Line Ratios				
C III λ1176/λ977	14.9	14.6	15.1	Vernazza (1977a)
	14.6	14.5	14.6	Dupree et al. (1977)
	14.4			Dufton et al. (1977)
N III λ772/λ989	14.5			
O V λ760/λ630	14.9	14.3	15.1	Vernazza (1977a)
	14.4			Dufton et al. (1977)
C III λ1247/λ1908	15.1			Nicolas (1977)
Si III λ1301/λ1296	15.3			Nicolas (1977)
O IV λ1404/λ1401	15.2			Nicolas (1977)
λ1407/λ1404	15.2			Nicolas (1977)
Energy Balance	14.5	14.3	14.7	Rosner et al. (1977); Withbroe (1977b)

* ξ is the assumed microturbulent velocity

TABLE II. ELECTRON PRESSURES IN DIFFERENT REGIONS

TECHNIQUE	Log P/k = log $N_e T$ CORONAL HOLE	QUIET REGION	ACTIVE REGION	SOURCE
CORONA				
Limb Observations	14.40	14.80		Mariska (1977)
Disk Observations	14.45	14.90	15.6	Mariska (1977); Withbroe (1977)
TRANSITION LAYER				
Optical Depths				
C II λ1335				
(ξ = 0)	$\gtrsim$14.2	$\gtrsim$14.2		Mariska (1977); Withbroe, Mariska (1976)
(ξ = 17 km/sec)	$\gtrsim$13.8	$\gtrsim$13.8		
C III λ977				
(ξ = 0)	$\gtrsim$14.1	$\gtrsim$14.5		Mariska (1977); Withbroe, Mariska (1976)
(ξ = 17 km/sec)	$\gtrsim$13.8	$\gtrsim$14.2		
Line Ratios				
C III λ1175/λ977	14.9	14.9	15.5	Vernazza (1977a)
N III λ772/λ989	14.5	14.5	15.1	Vernazza, Mason (1977)
O V λ760/λ629	14.9	14.9	15.8	Vernazza (1977a)
Mg IX λ439/λ368		14.5	15.0	Vernazza (1977a)
Energy Balance	14.4	14.5	15.5	Rosner et al. (1977); Withbroe (1977b)

the transition layer are accurate to only about a factor of 2 for all regions, the temperature gradients which vary as

$$\frac{dT}{dh} = \frac{P^2}{k^2T^2} \frac{1}{Q(T)} , \qquad (5)$$

are uncertain by a factor of about 4. Consequently, our empirical knowledge of the conductive flux in the transition layer, which is proportional to the temperature gradient, is also uncertain by a factor of 4.

This problem is particularly critical in the case of coronal holes. Some data, particularly line ratios, indicate that the electron pressure in the transition layer of coronal holes is approximately equal to that in quiet regions. This suggests that the temperature gradient in the transition layer of coronal holes is approximately the same as in quiet regions, since the differential emission measures for log T<5.9 in the two types of regions are approximately equal (see Figure 2). On the other hand, empirical data indicate that the electron pressure in the coronal layers of coronal holes is lower by a factor of 2 to 3 than in quiet regions. For a plane parallel model in hydrostatic equilibrium, this implies that the pressure in the transition layer is lower by a similar factor and that the temperature gradient is a factor of 5 to 10 shallower in coronal holes than in quiet regions (cf. Munro and Withbroe, 1972, Mariska 1977). For the upper transition layer and low corona (log T $\gtrsim$ 5.9) this has been confirmed directly by measurments of emission gradients at the limb measured in O VI λ1032 (Mariska 1977). There is also evidence that the height of the transition layer measured at the limb in transition layer lines from ions such as C III, O IV and O VI is larger than in quiet regions by about a factor of 5 (e.g. Tousey et al., 1973, Huber et al., 1974, Bohlin et al., 1975a). However, this effect could also be caused by differences in the EUV emission from spicules which are systematically larger in coronal holes than in quiet regions (Bohlin et al., 1975b, Withbroe et al., 1976).

Rosner and Vaiana (1977) suggest that it may be possible to keep the pressure in the transition layer of coronal holes comparable to that in quiet regions if one assumes that there is a rapid increase in the area of the transition layer between log T = 5.8 and 6.0. If so, it may be possible to account for all of the above mentioned observations by a model in which (1) the pressure in the lower transition layer is nearly the same as in quiet regions (thus satisfying line ratio measurements) and (2) the observed increase in height and thickness of the emission peaks at the limb observed in lines formed at T < 10^6 K is attributed to a combination of differences in the EUV spicular emission between coronal holes and quiet regions and to the rapid increase in cross sectional area of the transition layer above log T = 5.7. This problem clearly needs more theoretical and observational investigation.

For additional discussion of empirical models of the transition layer see reviews by Athay (1971, 1976), Jordan and Wilson (1971), Jordan (1975, 1976), Gabriel (1977), Withbroe and Noyes (1977), and references cited in these reviews.

3. Theoretical Models

The derivation of theoretical models for the transition layer has been discussed in a number of papers (e.g. Moore and Fung 1972, Shemeleva and Syrovatskii 1973, Landini and Monsignori Fossi 1975, McWhirter et al., 1975, Gabriel 1976, 1977, Kopp and Orrall 1976, Rosner and Vaiana 1977, Rosner et al., 1977). These models are based on the assumption of a net balance between the various energy sinks and sources in each atmospheric layer, that is

$$\nabla\cdot(F_r + F_c + F_m + F_g + F_k + F_e) = 0 \qquad (6)$$

where F_r is the radiative flux, F_c is the conductive flux, F_m is the mechanical energy flux, F_g is the gravitational potential energy flux, F_k is the kinetic energy flux and F_e is the enthalphy flux (see Gabriel 1977).

Let us consider first static steady state models which assume plane parallel geometry, models which require only the first three terms in equation (6). The simplest model of this type is one in which $\nabla\cdot F_m=0$ and where the gas pressure is constant. If $F_c >> F_r$, then $F_c \sim$ constant and the differential emission measure

$$Q(T) = \frac{P^2}{k^2T^2} \left(\frac{dT}{dh}\right)^{-1} = \frac{1.1\times10^{-6}\ P^2\ T^{1/2}}{F_c\quad k^2} \qquad (7)$$

varies as $T^{1/2}$. A curve of this type is plotted in Figure 3 as a dash-dot line. It does not fit the empirical curve (heavy solid line) very well, particularly below log T = 5.0. Equation (7) is based on thermal conductivities given by Ulmschneider (1970) and Nowak and Ulmschneider (1977) for log T > 4.3.

The empirical differential emission measure for log T < 5.0 contains important information concerning the energy balance in the lower transition layer and upper chromosphere. The variation of Q with temperature is very uncertain there due to the use of intensity relations (equation 2) which depend upon the use of a simple two-level atom. Empirical emission measures derived using equation (2) and intensities of neutral and singly ionized atoms could be systematically low due to the assumption that all atoms are in the ground state. The

values of Q(T) for these atoms could also be displaced to temperatures that are too high due to the neglect of the influence of temperature pleateaus, such as the one proposed to exist near T = 20,000 K, and use of simple ionization equilibrium calculations that neglect the influence of the radiation field, (e.g. Chipman 1971, Nussbaumer and Storey 1975, Lites et al., 1977). However, one can not escape the fact that at some temperature between log T = 4.0 and 5.0 the differential emission measure will be 1.5 to 2 orders of magnitude above that at log T = 5.0. This implies that the conductive flux drops by two orders of magnitude between the top of the transition layer (log T $\gtrsim$ 6.0) and the lower transition layer (log T < 5.0). Hence, if a static energy balance model is going to account for the observations, the transition layer must radiate away essentially all of the energy deposited in it by thermal conduction from the corona and by energy sources within the transition layer. This implies F_c (T_0) $\simeq$ 0 where $10^4 < T_0 < 10^5$ K (cf. Moore and Fung 1972, McWhirter et al., 1975, Rosner et al., 1977).

An alternate possibility is that the energy carried by thermal conduction into the lower transition layer and upper chromosphere can not be balanced by the radiative losses there. If this is the case, the material is heated, becomes convectively unstable and flows upward into the corona (cf. Kuperus and Athay 1967, Bessey and Kuperus 1970, Defouw 1970). As suggested by Moore and Fung (1972), Pye et al., (1977), Rosner et al., (1977) and others, this may be the mechanism by which the atmosphere reaches the state where F_c (T_0) $\simeq$ 0. If the rate of mechanical energy deposition increases, the coronal temperature will rise as will the downward conductive flux. If there is insufficient material in the transition layer to radiate all of the energy carried into the transition layer from the corona, material in the upper chromosphere will be evaporated by the excess conductive flux, increasing the radiative losses and thus reducing the conductive flux reaching the chromosphere. The evaporative process terminates when F_c (T_0) $\simeq$ 0. If the rate of mechanical energy deposition decreases, the transition layer will radiate away more energy than it receives, develop a thermal instability and lose material to the chromosphere. It will continue to lose material until the radiative losses become sufficiently low that the radiative, conductive and mechanical energy fluxes come into balance again. Because of the broad implications of this process in the flow of mass and energy between the chromosphere and corona, it should be investigated more throughly to determine its applicability to conditions in various solar regions.

On the basis of current empirical and theoretical results, it appears reasonable to assume F_c (T_0) $\simeq$ 0 for some value of temperature T_0 between 10^4 and 10^5 K and use this assumption in the derivation of theoretical models. In Figure 3 are plotted the differential emission measures calculated for two models based on this assumption and the assumption that the gas pressure is constant in the transition layer. One of these models (long-dash-line) assumes $\nabla \cdot F_m = 0$ in the transition layer and

the other (short-dash-line) that $\nabla \cdot F_m \neq 0$ and that the mechanical energy deposition per unit volume is constant throughout the transition layer and corona (Rosner et al., 1977).

Given the above mentioned uncertainties in the empirical differential emission measure curves, these models, particularly that of Rosner et al., appear to be in good agreement with the empirical differential emission measure curve for 5.0 < log T < 6.0. As indicated above, the large empirical values for Q(T) for log T < 5.0 may actually occur at lower temperatures (and thus bring the theoretical and empirical curves into better agreement) if there is a temperature plateau near log T = 4.3 as suggested by Chipman (1971), Vernazza et al., (1973), Lites et al., (1977) and others. Alternatively, log $T_0 \simeq 4.6$ instead of 4.3 as assumed in the models.

An important characteristic of energy balance models with F_c (T_0) $\simeq$ 0 is that they predict a relationship between the differential emission measure and pressure (cf. Moore and Fung, 1972, Landini and Monsignori Fossi 1975, McWhirter et al., 1975, Rosner et al., 1977, Withbroe 1977). One can demonstrate that this relation is

$$Q(T) = \frac{P}{k}\left[1.1\times10^{-6}T\right]^{1/2}\left[2\int_{T_0}^{T}\phi(T)T^{1/2}dT\right]^{-1/2} \qquad (8)$$

where $\phi(T)$ is the radiative loss function. Hence, if the differential emission measure in the transition layer can be determined, equation (8) can be used to derive the electron pressure. Electron pressures evaluated using this formula are given in Tables I and II. These pressures agree with those determined empirically to within the uncertainties of the latter, namely a factor of about 2. This agreement is additional evidence supporting the hypothesis that static energy balance models with F_c (T_0) $\simeq$ 0 may provide a good representation of the physical conditions in typical quiet and active regions.

At some height in the transition layer, models based on the assumption of constant pressure will become inadquate. In hydrostatic equilibrium models for quiet regions the pressure begins to decrease with height at heights above that corresponding to temperatures greater than about 5×10^5 to 10^6 K, depending on the model. The dotted line in Figure 3 is the variation of differential emission measure predicted by an energy balance model based on the assumption of hydrostatic equilibrium in a plane parallel atmosphere (McWhirter et al., 1975). This model does not fit the empirical differential emission measure curve very well, particularly in the corona where log T $\gtrsim$ 6.0. However, Gabriel (1976, 1977) has shown that if one introduces the effects of the channeling of the conductive flux by the magnetic field associated with the network, one can dramatically change the behavior of a theoretical differential emission measure curve. This is shown

by the light solid line in Figure 3 which is the differential emission measure curve predicted for a hydrostatic equilibrium energy balance model with the magnetic configuration illustrated in Figure 4.

Rosner and Vaiana (1977) have also demonstrated that changing the cross-sectional area of the atmosphere as a function of height can significantly modify the variation of the differential emission measure with temperature. Their model assumes that the atmosphere is confined to a radially oriented magnetic flux tube whose cross-sectional area can change with height. Increasing the cross-sectional area A by a factor of 2 in such a model decreases the conductive flux by a factor of 2 and increases the differential emission measure Q by a factor of 4, since $Q \sim A/F_c$.

The empirical differential emission measure curves for quiet regions and active regions given in Figures 1 and 2 and similar curves derived from OSO data (Withbroe 1975) imply that, if the transition layer and corona are contained in radially oriented flux tubes, then the cross-sectional areas of these tubes increases rapidly between log T = 5.7 and log T = 6.0. This is in good agreement with the observed spatial variation of the intensities of EUV emission lines formed at different temperatures in the quiet sun as is illustrated in Figure 5. The emission from spectral lines formed in the chromosphere (Ly α, C II) and transition layer (C III, O IV, O VI) is concentrated in the network, while the emission from the coronal line (Mg X) has a much more uniform distribution.

The importance of the configuration of the magnetic field can not be over-emphasized. Withbroe and Gurman (1973) found from an analysis of a large number of EUV spectra from OSO-6 (35 arc sec spatial resolution), that empirical models for the transition layer based on the assumption of plane parallel geometry yielded the relationship that the conductive flux $F_c \sim p^{1.8}$ for $P \leq 0.4$ dyn/cm^2 and $F_c \sim$ constant for greater pressures. They pointed out that this is in disagreement with plane parallel energy balance models (which predict $F_c \sim P$). It now appears that the reason for the disagreement is the assumption of plane parallel geometry in both the empirical models derived by Withbroe and Gurman and the theoretical models with which they were compared. A useful approach in the derivation of models would be to assume the validity of the static energy balance models and use these models in conjunction with the observations to derive information about the configuration of the magnetic fields in the transition layer. Gabriel's (1976, 1977) models provide one method of doing this.

4. Inhomogeneties and Mass Flows

In the development of models for the transition layer one must take into consideration several types of inhomogeneties.

Differences in the physical conditions above various areas of the solar surface appear to be intimately related to the configuration and strength of the magnetic fields in these areas (see review by Withbroe and Noyes 1977). We have already mentioned the importance of the magnetic field configuration associated with the chromospheric network. If the fields originating in the network are closed on a large scale (significant fraction of a solar radius), then the region will most likely become a so-called quiet region. If the field configuration is open, the region will become a coronal hole. Differences in the temperature-density structure in transition layers of coronal holes and quiet regions can be attributed to differences in the mass and energy carried away from the corona by the solar wind. In regions with small scale (less than few tenths $R_\odot$) closed configurations, such as active regions and coronal bright points, there is enhanced coronal heating which required larger radiative and conductive energy losses in the transition layer and hence steeper temperature gradients and higher densities than in quiet regions. In active regions one should construct models for individual magnetic flux tubes, since the physical conditions can change dramatically from one flux tube to another.

In quiet regions mean models do make a certain amount of sense, because on a large scale (few tenths $R_\odot$ or larger) the physical conditions in the transition layer do not appear to change a great deal from one region to another, the small scale structure appears to be more important. In addition to the network, one must take into consideration the fine scale structure associated with spicules and small scale features in the network that have closed magnetic field configurations. Unfortunately the presently available data do not allow one to unambigously determine whether or not spicules are an important source of EUV radiation. Although spicules cover only a few percent of the solar surface, they may emit a significant fraction of the EUV emission observed in lines formed between 10^4 and 10^6 K. Some observational evidence suggests that the fraction of the EUV emission originating from spicules is small (e.g. Burton et al., 1973) while other observations (Brueckner and Nicolas 1973, Withbroe and Mariska 1976, Mariska 1977) indicates that a significant fraction, as much as 20% or more in the quiet sun and 50% or more in coronal holes, may originate in spicules. If the spicular contribution is small, less than 10% or 20%, then one does not make a very serious error if one ignores spicular emission when constructing a model for the transition layer. If the spicular contribution is large, 50% or more, then models derived without taking spicules into consideration will give a poor representation of the physical conditions in the transition layer. Observations made with high spatial resolution ($\lesssim$ arc sec) are required to measure the EUV emission from spicules to provide a definitive answer concerning their importance as a source of EUV radiation.

A more serious problem associated with small scale inhomogeneties is the mass flow associated with these features.

Observations from OSO-8, Skylab and rocket experiments indicate that there are systematic downflows in the transition layer with velocities of 2 to 15 km/sec (Doschek et al., 1976a, Lites et al., 1976, Shine et al., 1976, White 1977). These flows could result from cooling of coronal material that becomes thermally unstable, cools, increases in density and falls into the chromosphere (Foukal 1976, Pneuman and Kopp 1977). As Pneuman and Kopp suggest, the energy carried by these flows could be an important factor in the energy balance of the transition layer. However, if the observed red shifts are not caused by infalling coronal material, but result from the downward motions of spicules which are brighter in EUV lines when descending than when ascending, then the importance of the apparent downflows in the energy balance will be reduced significantly.

Another type of inhomogenety is that associated with the broadening of EUV transition layer lines whose widths correspond to non-thermal velocities of about 5 to 25 km/sec depending on the temperature of formation (e.g. Boland et al., 1973, 1975, Doschek et al., 1976b, Feldman et al., 1975, 1976a, 1976b, Moe and Nicolas 1977). Boland et al. (1973, 1975), McWhirter et al. (1975), Jordan (1976) and others have suggested that this non-thermal broadening is caused by wave motions. One must take account of the dynamic pressure due to these motions when constructing models for the transition layer. Gabriel (1977) finds that the non-thermal contribution to the total pressure reaches a maximum of about 50% at log T = 4.4 and decreases rapidly at higher and lower temperatures. McWhirter et al. (1975), Gabriel (1977), and Rosner and Vaiana (1977) discuss some of the problems associated with including the effects of wave pressure in transition region models.

5. Summary and Conclusions

Recent empirical and theoretical investigations of the structure of the transition layer suggest that energy balance models may be able to satisfactorily explain the differential emission measures and densities inferred from EUV observations providing the assumption of plane parallel geometry is discarded. These studies also demonstrate that the configuration of the magnetic field has major effects of the temperature-density structure of the transition layer and that these effects should be incorporated into any model intending to represent the physical conditions in the transition layer.

The development of improved models for the transition layer required progress in five areas: (1) the calculation of theoretical line intensities, (2) knowledge of the magnetic field configurations, (3) determination of the relative contributions of various types of inhomogeneties to the EUV emission to the transition layer, (4) determination of the origin and magnitude of the mass flows and (5) determination

of the causes of the non-thermal line broadening. Existing OSO-8, rocket and Skylab data undoubtedly contain a wealth of information that can be used and is being used to attack these problems. However, we clearly need improved observations made with simultaneous high spatial, spectral and time resolutions if we are going to resolve these problems. New experiments which may be flown on Shuttle such as the proposed 1.25 meter aperture optical telescope (SOT), new UV, EUV and XUV experiments with spatial resolutions of the order of 0.3 to 1 arc sec, and the already existing HRTS experiment of Naval Research Laboratory (Brueckner et al., 1976) could provide the empirical data needed to eliminate the major remaining sources of uncertainty in our models for the transition layer.

Acknowledgements

I wish to thank C. Jordan, J. Mariska, R. Rosner, and J. Vernazza for stimulating discussions on transition region models. This work was supported in part by NASA through contract NAS 5-3949 and Air Force Geophysical Laboratory by contract F19628-76-C-0281.

References

Allen, J.W. and Dupree, A.K. 1969, Astrophys. J. 155, 27.

Antiochos, S.K. and Sturrock, P.A. 1976, Solar Phys. 49, 359.

Athay, R.G. 1971, in Physics of the Solar Corona, C.J. Macris (ed.), (Reidel, Dordrecht, Holland), p. 36.

Athay, R.G. 1976, The Solar Chromosphere and Corona: Quiet Sun, (Reidel, Dordrecht, Holland).

Bely, O. 1966, Proc. Phys. Soc., 88, 587.

Bessey, R.J. and Kuperus, M. 1970, Solar Phys., 12, 216.

Bohlin, J.D., Sheeley, N.R., and Tousey, R. 1975a, in A.C. Strickland (ed.), Space Research XV, (Akademie-Verlag, Berlin) p. 651.

Bohlin, J.D., Vogel, S.N., Purcell, J.D., Sheeley, N.R., Jr., Tousey, R. and Van Hoosier, M.E. 1975b, Astrophys. J. 197, L133.

Boland, B.C., Dyer, E.P., Firth, J.C., Gabriel, A.H., Jones, B.B., Jordan, C., McWhirter, R.W., Monk, P. and Turner, R., 1975, Mon. Not. Roy. Astron. Soc., 171, 697.

Boland, B.C., Engstrom, S.F.T., Jones, B.B. and Wilson, R. 1973, Astron. Astrophys. 22, 161.

Brueckner, G.E. and Nicolas, K.R. 1973, Solar Phys. 29, 301.

Brueckner, G.E., Nicolas, K.R., Bartoe, J.D.F. and Van Hoosier, M.E. 1976, Bull. Amer. Astron. Soc. 8, 345.

Burton, W.M., Jordan, C., Ridgeley, A. and Wilson, R. 1973, Astron. Astrophys. 27, 101.

Chipman, E.G. 1971, Ph.D. Thesis, Harvard University.

Cox, D.P. and Tucker, W.H. 1969, Astrophys. J. 157, 1157.

Defouw, R.J. 1970, Solar Phys. 14, 42.

Doschek, G.A., Feldman, U. and Bohlin, J.D. 1976a, Astrophys. J. 205, L177.

Doschek, G.A., Feldman, U., Van Hoosier, M.E. and Bartoe, D.F. 1976b, Astrophys. J. Suppl. 31, 417.

Dufton, P.L., Berrington, K.A., Burke, P.G.. and Kingston, A.E. 1977, Astron. Astrophys., in press.

Dupree, A.K. 1972, Astrophys. J. 178, 527.

Dupree, A.K., Foukal, P.V. and Jordan, C. 1977, Astrophys. J. 209, 621.

Dupree, A,K. and Wood, A.T. 1969, private communication.

Feldman, U., Doschek, G.A. and Tousey, R. 1975 Astrophys. J. 202, L147.

Feldman, U., Doschek, G.A. and Patterson, N.P. 1976a Astrophys. J. 209, 270.

Feldman, U., Doschek, G.A., Van Hoosier, M.E. and Purcell, J.D. 1976b, Astrophys. J. Suppl. 31, 445.

Foukal, P.V. 1976, Astrophys. J. 210, 575.

Gabriel, A.H. 1976, Phil. Trans. Roy. Soc. A. 281, 339.

Gabriel, A.H. 1977, The Energy Balance and Hydrodynamics of the Solar Chromosphere and Corona, (G. de Bussac, Clermont-Ferrand) p. 375.

Huber, M.C.E., Foukal, P.V., Noyes, R.W., Reeves, E.M., Schmahl, E.J., Timothy, J.G., Vernazza, J.E. and Withbroe, G.L. 1974, Astrophys J. 194, L115.

Jordan, C. 1975, in S.R. Kane (ed.), Solar Gamma X- and EUV Radiation, (Reidel, Dordrecht, Holland), p. 109.

Jordan, C. 1976, Phil. Trans. Roy. Soc. Lon. A. 281, 391.

Jordan, C. 1977, private communication.

Jordan, C. and Wilson, R. 1971, in Physics of the Solar Corona, C.J. Macris (ed.), (Reidel, Dordrecht, Holland), p. 219.

Kopp, R.A. and Orrall, F.Q. 1976, Astron. Astrophys. 53, 363.

Kopp, R.A. and Orrall, F.Q. 1977, in R.M. Bonnet, P. Delache (eds.), The Energy Balance and Hydrodynamics of the Solar Chromosphere and Corona (G. de Bussac, Clermont-Ferrand), p. 457.

Kuperus, M. and Athay, R.G. 1967, Solar Phys. 1, 361.

Landini, M. and Monsignori Fossi, B.C. 1975, Astron. Astrophys. 42, 213.

Lites, B.W., Bruner, E.C., Jr., Chipman, E.G., Shine, R.A., Rottman, G.J., White, O.R. and Athay, R.G. 1976, Astrophys. J. 210, L111.

Lites, B.W., Shine, R.A. and Chipman, E.G. 1977, Astrophys. J., in press.

Mariska, J.T. 1977, Ph.D. Thesis, Harvard University.

McWhirter, R.W.P., Thonemann, P.C., and Wilson, R. 1975 Astron. Astrophys. 40, 63.

Moe, O. and Nicolas, K.R. 1977, Solar Phys., in press.

Moore, R.L. and Fung, P.C.W. 1972, Solar Phys. 23, 78.

Munro, R.H., Dupree, A.K. and Withbroe, G.L. 1972, Solar Phys. 19, 347.

Munro, R.H. and Withbroe, G.L. 1972, Astrophys. J. 176, 511.

Nicolas, K.R. 1977, Ph.D. Thesis, University of Maryland.

Nowak, T. and Ulmscheider, P. 1977, Astron. Astrophys., in press.

Noyes, R.W., Dupree, A.K., Huber, M.C.E., Parkinson, W.H., Reeves, E.M. and Withbroe, G.L. 1972, Astrophys. J. 178, 515.

Nussbaumer, H. and Storey, P.J. 1975, Astron. Astrophys. 44, 321.

Pneuman, G.W. and Kopp, R.A. 1977, Astron. Astrophys. 55, 305.

Pottasch, S.R. 1964, Space Sci. Rev. 3, 816.

Pottasch, S.R. 1967, Bull. Astron. Inst. Neth. 19, 113.

Pye, J.P., Evans, K.P., Hutcheon, R.J., Gerassimenko, M., Davis, J.M., Krieger, A.S. and Vesecky, J.F. 1977, Astron. Astrophys., in press.

Raymond, J.C., Cox, D.P. and Smith, B.W. 1976, Astrophys. J. 204, 290.

Rosner, R., Tucker, W.H. and Vaiana, G.S. 1977, Astrophys. J. in press.

Rosner, R. and Vaiana, G.S. 1977, Astrophys. J. 216, 141.

Shemeleva, O.P. and Syrovatskii, S.I. 1973, Solar Phys. 33, 341.

Shine, R.A., Roussel-Dupre, D., Bruner, E.C., Jr., Chipman, E.G., Lites, B.W., Rottmann, G.J., Athay, R.G. and White, O.R., 1976, Astrophys. J. 210, L106.

Tousey, R., Bartoe, J.D.F., Bohlin, J.D., Brueckner, G.E., Purcell, J.D., Scherrer, V.E., Sheeley, N.R., Jr., Schmacher, R.J. and Van Hoosier, M.E. 1973, Solar Phys. 33, 265.

Ulmschneider, P. 1970, Astron. Astrophys. 4, 144.

Vernazza, J.E. 1977a, presented at IAU Colloquium No. 43, "Ultraviolet and X-ray Spectroscopy of Astrophysical and Laboratory Plasmas," London.

Vernazza, J.E., 1977b, private communication.

Vernazza, J.., Avrett, E.H. and Loeser, R. 1973, Astrophys. J. 184, 605.

Vernazza, J.E. and Mason, H. 1977, to be submitted to Astrophys. J.

Vernazza, J.E. and Reeves, E.M. 1977, Astrophys. J., in press.

White, O.R. 1977, in R.M. Bonnet, P. Delache (eds.), The Energy Balance and Hydrodynamics of the Solar Chromosphere and Corona (G. de Bussac, Clermont-Ferrand), p. 75.

Withbroe, G.L. 1970, Solar Phys. 11, 42.

Withbroe, G.L. 1975, Solar Phys. 45, 301.

Withbroe, G.L. 1976, presented at Annual Meeting of AGU. Center for Astrophysics Preprint No. 524.

Withbroe, G.L. 1977, in R.M. Bonnet, P. Delache (eds.), The Energy Balance and Hydrodynamics of the Solar Chromosphere and Corona (G. de Bussac, Clermont-Ferrand), p. 421.

Withbroe, G.L. 1977b, to be submitted to Astrophys. J.

Withbroe, G.L. and Gurman, J.B. 1973, Astrophys. J. 183, 279.

Withbroe, G.L., Jaffe, D.T., Foukal, P.V., Huber, M.C.E., Noyes, R.W., Reeves, E.M., Schmahl, E.J., Timothy, J.G. and Vernazza, J.E. 1976, Astrophys. J. 203, 528.

Withbroe, G.L. and Mariska, J.T. 1976, Solar Phys. 48, 21.

Withbroe, G.L. and Noyes, R.W. 1977, Ann. Rev. Astron. Astrophys. 15, 363.

Zirker, J.G. 1977, in R.M. Bonnet, P. Delache (eds.), The Energy Balance and Hydrodynamics of the Solar Chromosphere and Corona (G. de Bussac, Clermont-Ferrand), p. 421.

Figure Captions

Figure 1. Differential emission measure Q as a function of temperature. Points, emission measures from spectral lines with $\lambda > 912$ Å. Crosses, emission measures for lines with $\lambda < 912$ Å. Squares, spectral lines from lithium and sodium isoelectronic sequences. Solid line, iterative solution using lines with $\lambda > 912$ Å and strongest lines in lithium sequence.

Figure 2. Empirical differential emission measures for representative regions derived from spectra compiled by Vernazza and Reeves.

Figure 3. Differential emission measures versus temperature from empirical data (heavy solid line) for the quiet sun (see Figure 1) and from various theoretical models. The curve for $F_c(T_0) = 0$, heating throughout, is from the model of Rosner et al., (1977). Emission measures from the model of McWhirter et al. have been decreased by a factor of 1.75 in order to obtain a better fit to the empirical curve.

Figure 4. Magnetic field configuration associated with the network and temperature contours from Gabriel's (1976) model for the transition region and low corona in a quiet region.

Figure 5. EUV spectroheliograms of a quiet region near sun center. Data from Harvard Skylab experiment.

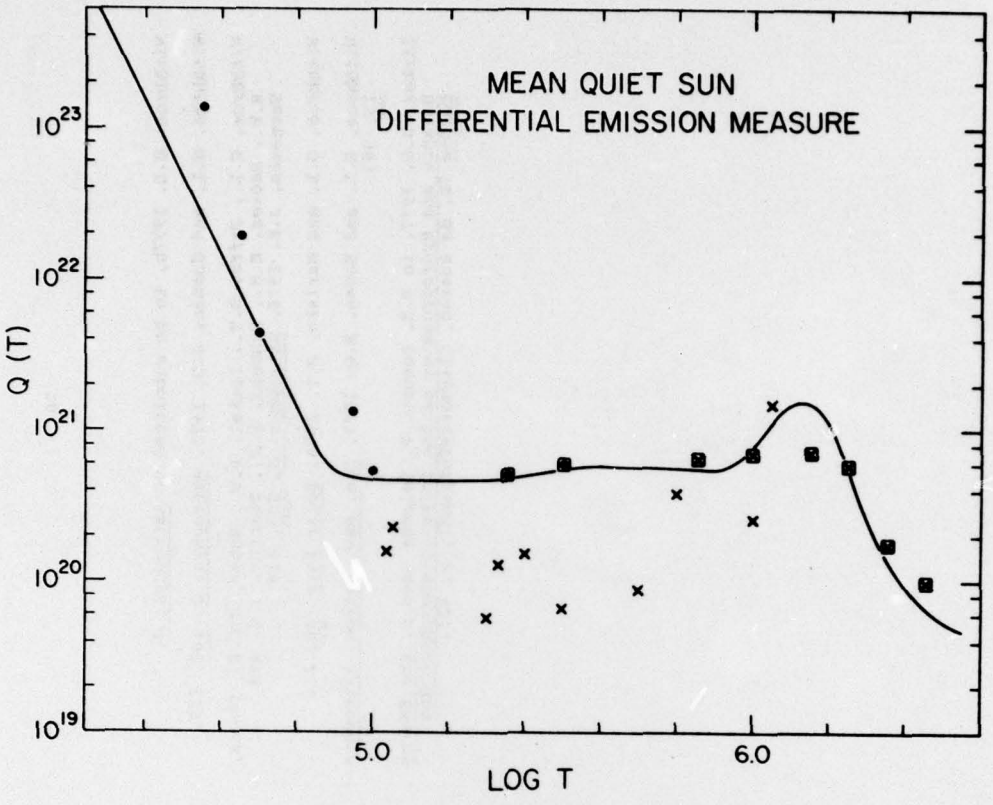

Figure 1

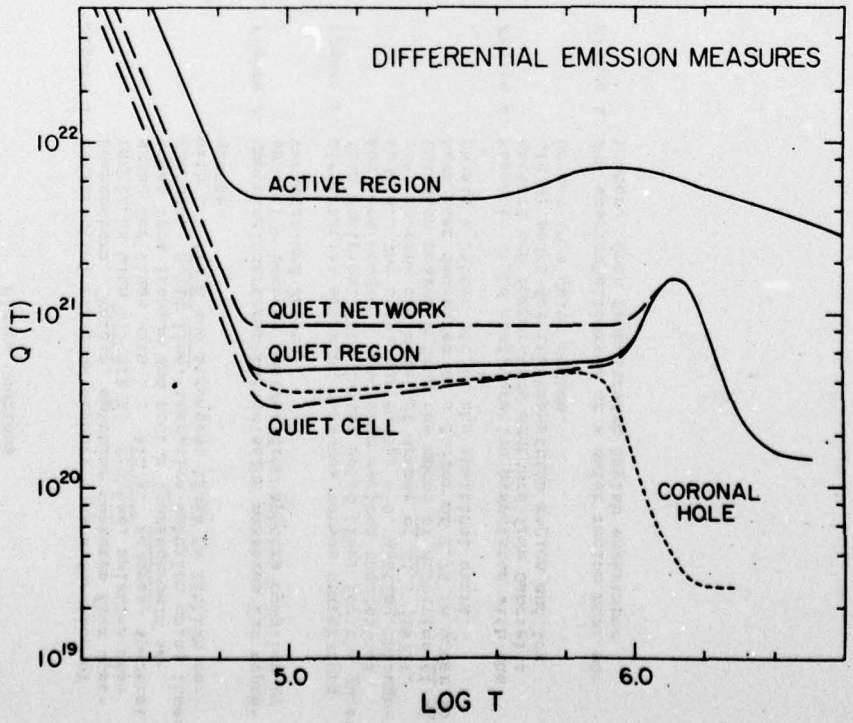

Figure 2

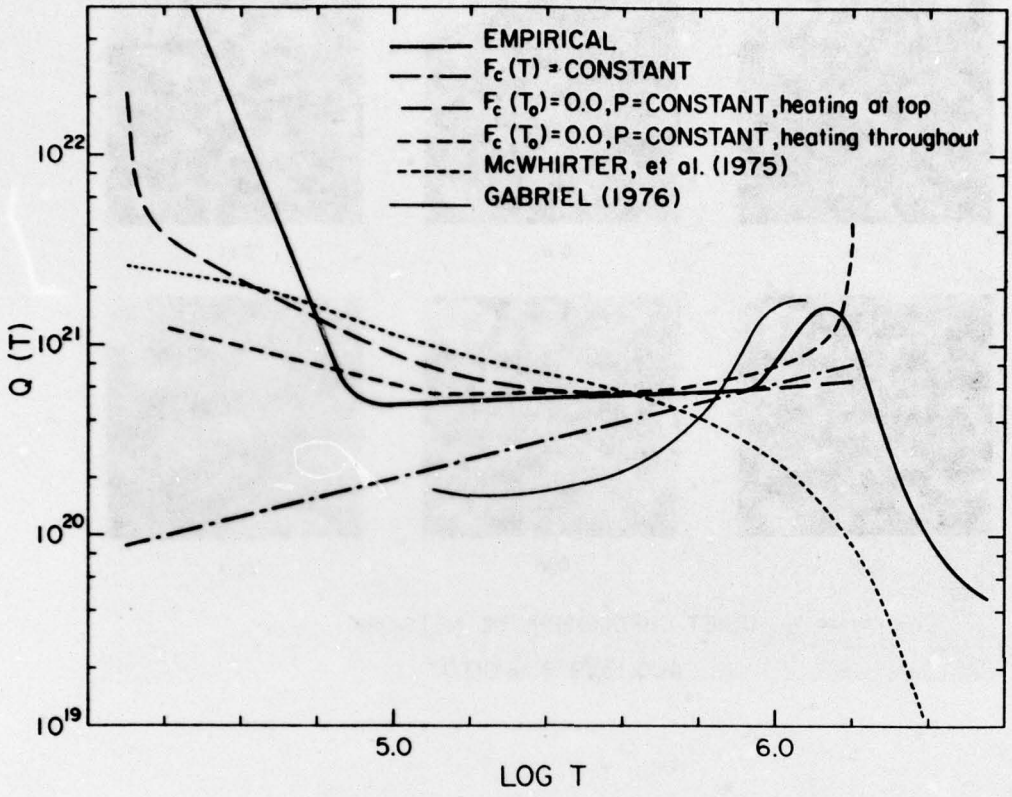

Figure 3

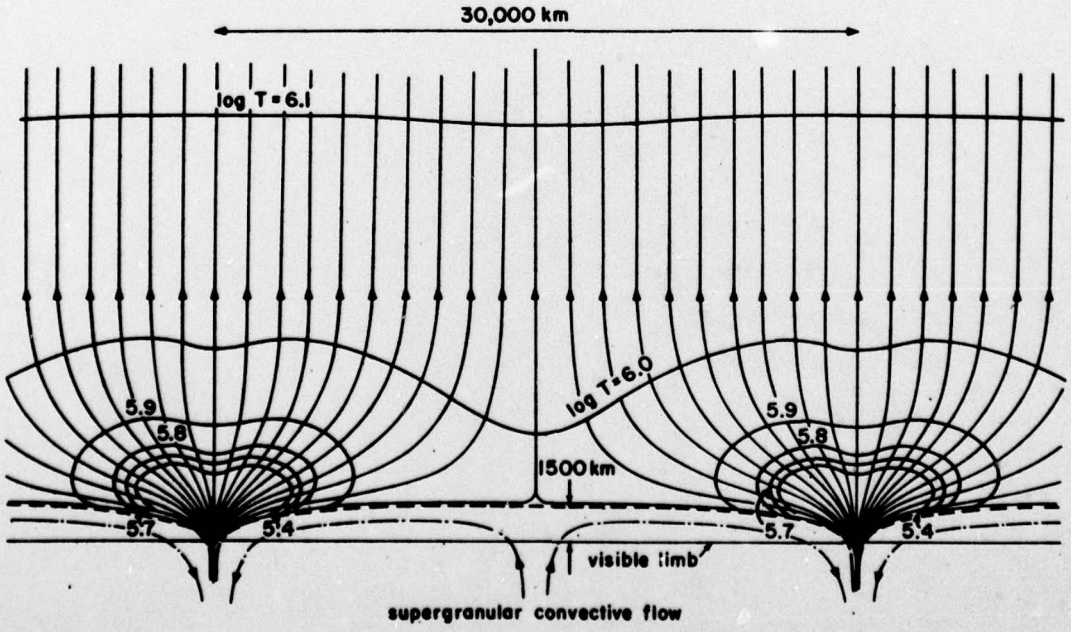

Figure 4

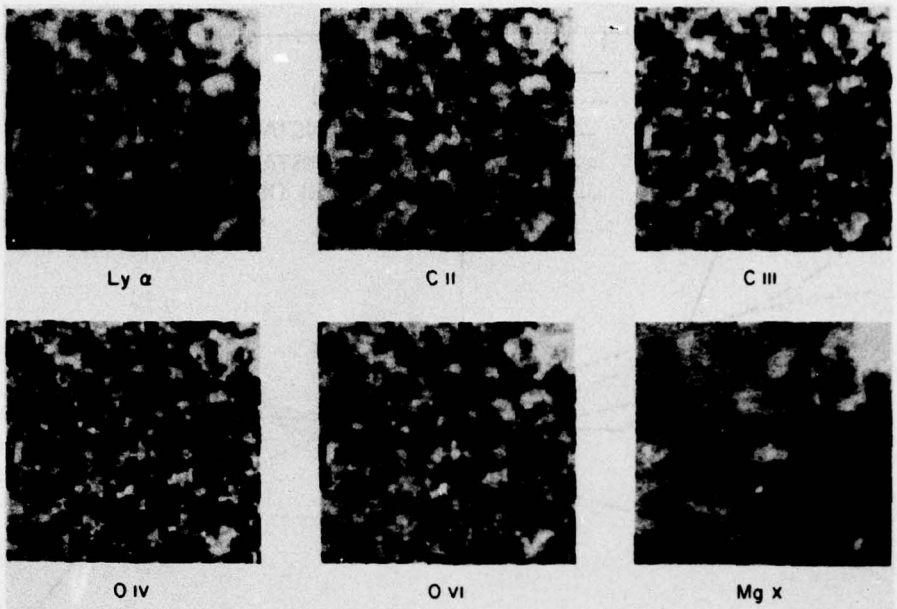

Figure 5 QUIET CHROMOSPHERIC NETWORK

AUG 13, 1973 16:00 UT